NEUROSCIENCE

Short-term acute bright light exposure induces a prolonged anxiogenic effect in mice via a retinal ipRGC-CeA circuit

Ge Wang[1], Yun-Feng Liu[1], Zhe Yang[1], Chen-Xi Yu[1], Qiuping Tong[1], Yu-Long Tang[1], Yu-Qi Shao[1], Li-Qin Wang[1], Xun Xu[2], Hong Cao[1], Yu-Qiu Zhang[1], Yong-Mei Zhong[1], Shi-Jun Weng[1]*, Xiong-Li Yang[1]*

Light modulates mood through various retina-brain pathways. We showed that mice treated with short-term acute bright light exposure displayed anxiety-related phenotypes in a prolonged manner even after the termination of the exposure. Such a postexposure anxiogenic effect depended upon melanopsin-based intrinsically photosensitive retinal ganglion cell (ipRGC) activities rather than rod/cone photoreceptor inputs. Chemogenetic manipulation of specific central nuclei demonstrated that the ipRGC–central amygdala (CeA) visual circuit played a key role in this effect. The corticosterone system was likely to be involved in this effect, as evidenced by enhanced expression of the glucocorticoid receptor (GR) protein in the CeA and the bed nucleus of the stria terminalis and by the absence of this effect in animals treated with the GR antagonist. Together, our findings reveal a non-image forming visual circuit specifically designed for "the delayed" extinction of anxiety against potential threats, thus conferring a survival advantage.

INTRODUCTION

Anxiety disorder is the most prevailing mental disorder, affecting 7.3% of the global population (*1*), whereas anxiety itself is a beneficial adaptive response in all species, allowing the assessment of potential threats and keeping an organism alert to increase survival (*2*). There is mounting evidence that anxiety levels could be substantially modulated by lighting conditions (*3*–*5*). For example, nightly exposure to dim light at early life leads to anxiety-like behaviors in adult mice (*6*); meanwhile, decreased daytime illumination for 2 weeks has an anxiogenic effect on diurnal rats (*7*). In addition to the aforementioned chronic effects, a few studies also revealed acutely induced anxiety-like symptoms during bright light exposure, which were characterized by longer latency to enter the open arena and lower number of entries in the defensive withdrawal test in rats (*8*) and by abruptly reduced time in the center in the open-field test (OFT) in mice (*9*). However, it is unclear whether such an anxiogenic effect is prolonged, remaining even after the removal of light exposure, and if so, how long such postexposure anxiety-like behaviors could last and what kind of visual circuit(s) underlie it.

Beyond rod and cone photoreceptors, a small subset of retinal ganglion cells (RGCs) that detect ambient illumination levels, named intrinsically photosensitive RGCs (ipRGCs), can be directly excited by light due to the expression of a unique photopigment, melanopsin (*10*, *11*). Initially, ipRGCs were found to be involved in the so-called non-image forming (NIF) visual functions, such as photic regulation of circadian rhythms and pupillary light reflex (*12*–*14*), but subsequent studies have shown that ipRGCs project to a broad range of brain targets, modulating various non-visual functions such as body temperature (*15*), sleep and arousal (*15*–*20*), learning (*21*, *22*), memory performance (*23*), and affective behaviors including anxiety (*21*, *22*, *24*, *25*). Specifically, ipRGCs innervate several brain regions, which are shown to underlie anxiety, such as the lateral habenula, the bed nucleus of the stria terminalis (BNST), and the central/medial amygdala (*26*–*28*). Furthermore, anxiety-like behaviors have been observed in mice with chemogenetic selective activation of ipRGCs (*29*). Together, these results support the involvement of ipRGCs in light-induced anxiety-like behaviors.

In this study, we showed that C57BL/6 mice treated with short-term (25 min) acute bright light exposure displayed anxiety-like behaviors, which could be observed for at least 20 min after the termination of exposure. Experiments further showed that this anxiety-like behavior was driven by increased melanopsin-driven ipRGC inputs to central amygdala (CeA), and associated with up-regulated corticosterone (CORT) system activity. This response allows animals to maintain alertness for a considerably long period when encountering potential threats associated with high ambient illumination levels, thereby minimizing risks and helping survival.

RESULTS

Short-term acute bright light exposure causes prolonged postexposure anxiety-like behaviors

All behavioral tests were carried out during the nocturnal active phase [zeitgeber time (ZT) 14 to ZT17]. Given the marked persistence of melanopsin-based photoresponse and its slow recovery from bleaching (*30*–*32*), all animals were dark-adapted for >26 hours before light pulse application to uncouple any behavioral changes from recent lighting history. C57BL/6 mice were exposed to

[1]State Key Laboratory of Medical Neurobiology and MOE Frontiers Center for Brain Science, Institutes of Brain Science, Fudan University, Shanghai, China. [2]Department of Ophthalmology, Shanghai General Hospital, National Clinical Research Center for Eye Diseases, Shanghai Key Laboratory of Ocular Fundus Diseases, Shanghai Engineering Center for Visual Science and Photomedicine, Shanghai Engineering Center for Precise Diagnosis and Treatment of Eye Diseases, Shanghai, China.
*Corresponding author. Email: xlyang@fudan.edu.cn (X.-L.Y.); sjweng@fudan.edu.cn (S.-J.W.)

1000-lux full-field white light for 25 min. After light pulse removal, the animals were redark-adapted for 60 s and then challenged with the OFT or elevated plus maze (EPM) test in darkness under infrared illumination (Fig. 1A). This paradigm ensured that behavioral responses were tested in a physiologically "active" status, rather than in the "resting" status caused by longer light exposure; moreover, it allowed us to evaluate the prolonged, postexposure effects of light.

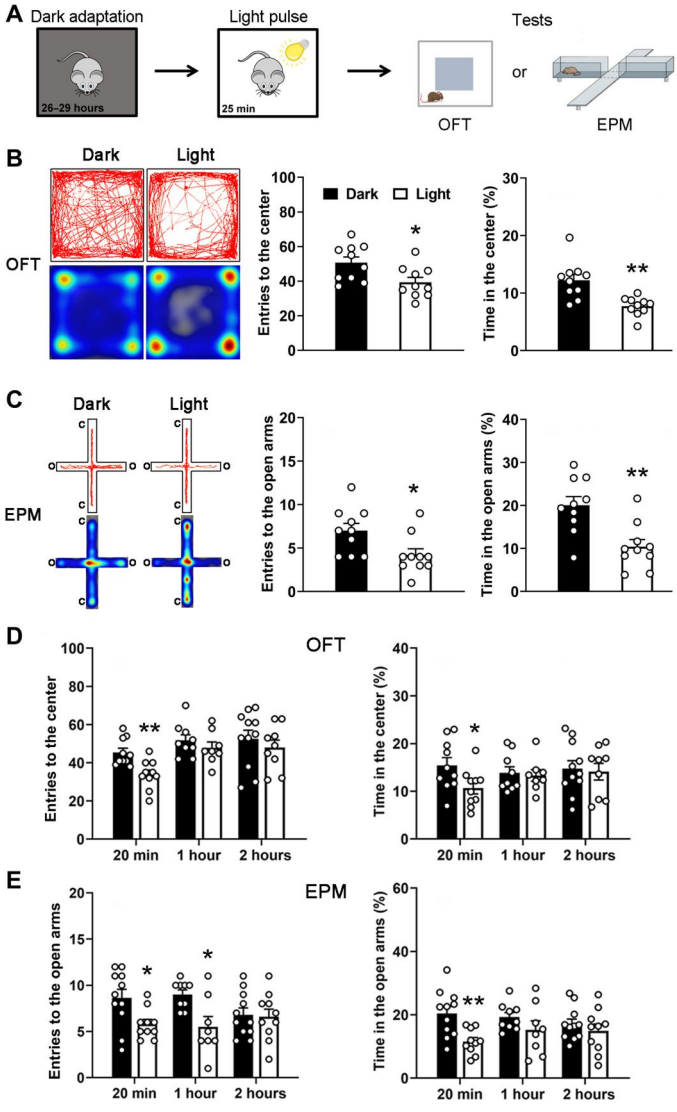

Fig. 1. Short-term acute bright light exposure resulted in prolonged postexposure anxiety-like behaviors in C57BL/6 mice. (**A**) Flow diagram showing the experimental procedures for investigating the light-induced anxiety-like behaviors. (**B** and **C**) Representative tracks/heat maps (left) and pooled data (right) showing that previous 25-min light pulse treatment at 1000 lux significantly reduced the time spent in/number of entries to the center [open-field test (OFT) (B)] and open arm [elevated plus maze (EPM) (C)]. *$P < 0.05$; **$P < 0.01$, unpaired *t* test; $n = 10$ in each group for both tests. (**D** and **E**) Bar charts illustrating the persistence of light-induced anxiety-like behaviors, which remained at 20 min after the removal of the light pulse (1000 lux, 25 min) as revealed by either the OFT (D) or EPM (E) but gradually disappeared within 2 hours. *$P < 0.05$; **$P < 0.01$, unpaired *t* test; $n = 8$ to 11. In all bar charts, data are presented as the means ± SEM.

Compared to control mice without light pulse treatment (denoted "dark group"), light pulse–treated mice (denoted "light group") exhibited reduced interest in exploring the central region in the OFT ($P = 0.017$ for center entries and $P = 0.001$ for center time; Fig. 1B) and significantly more thigmotaxis ($P = 0.001$; fig. S1A). Consistently, in the EPM, light group showed decreased number of entries to, and time spent in, the open arms compared with dark group ($P = 0.020$ for open entries and $P = 0.002$ for open time; Fig. 1C). Moreover, similar results were obtained at ZT2 to ZT5 (>14 hours of dark adaptation) (fig. S2), suggesting little diurnal variation of this light-induced effect. In addition, the anxiolytic agent estazolam, intraperitoneally applied 1 to 2 hours before light pulse treatment, completely abolished such anxiety-like behaviors, validating that the phenotypes observed were associated with increased anxiety (fig. S3). Collectively, these results strongly suggest the emergence of prolonged anxiety-like behaviors following the 1000-lux light pulse administration.

The irradiance-response profile of the anxiety-like behaviors was explored with three additional light intensities: 150, 600, and 3000 lux (fig. S4). Whereas a 150-lux pulse did not significantly affect activity preferences in both the OFT and EPM ($P > 0.05$ for all parameters analyzed), after the 600-lux light treatment, the time the mice spent in the center and open arms became less ($P = 0.025$ and 0.043, respectively), suggesting an irradiance-dependent feature.

After a 3000-lux light pulse treatment, despite of decreased number of entries to/time spent in the center (OFT) and open arms (EPM) (fig. S4, A to C), the mice exhibited a significantly reduced total distance traveled and an attenuated movement velocity ($P = 0.030$ in both cases; fig. S4D), suggesting severely perturbed locomotor activity. On the basis of these data, the illumination level of 1000 lux, which was effective in evoking the prolonged anxiety-like behaviors, but without causing locomotor inhibition, was used for all these experiments throughout the study.

The persistence of anxiogenic effect was investigated by conducting the OFT and EPM tests at various intervals after a 25-min light pulse application. Compared to dark group, light group showed significantly increased anxiety-like behaviors revealed at 20 min after light pulse removal ($P = 0.002$ for center entries, $P = 0.034$ for center time, $P = 0.017$ for open entries, and $P = 0.003$ for open time; Fig. 1, D and E). Unexpectedly, in the EPM, a significantly lower number of entries to open arms were still revealed in light group than in dark group even at 1 hour after light pulse removal ($P = 0.017$; Fig. 1E). At 2 hours after removal of the light pulse, the results obtained in the two groups were comparable in all behavioral parameters analyzed (all $P > 0.05$; Fig. 1, D and E), suggesting the complete extinction of the anxiogenic effect.

Rod/cone inputs are less important for light-induced anxiety-like behaviors

To characterize the photoreceptor inputs that drive the prolonged anxiety-like behaviors, we first injected (intraperitoneally) C57BL/6 mice with *N*-methyl-*N*-nitrosourea (MNU; 65 mg/kg), a direct-acting alkylating agent inducing rapid and specific rod/cone photoreceptor apoptosis (*33*). At 1 week after injection, the immunosignals of rhodopsin (rod marker) and peanut agglutinin (PNA) (cone marker) viewed from retinal sections were both extremely weak, and virtually lost, in MNU-injected animals (Fig. 2, A and B), suggesting the severe ablation of rod/cone photoreceptors. Furthermore,

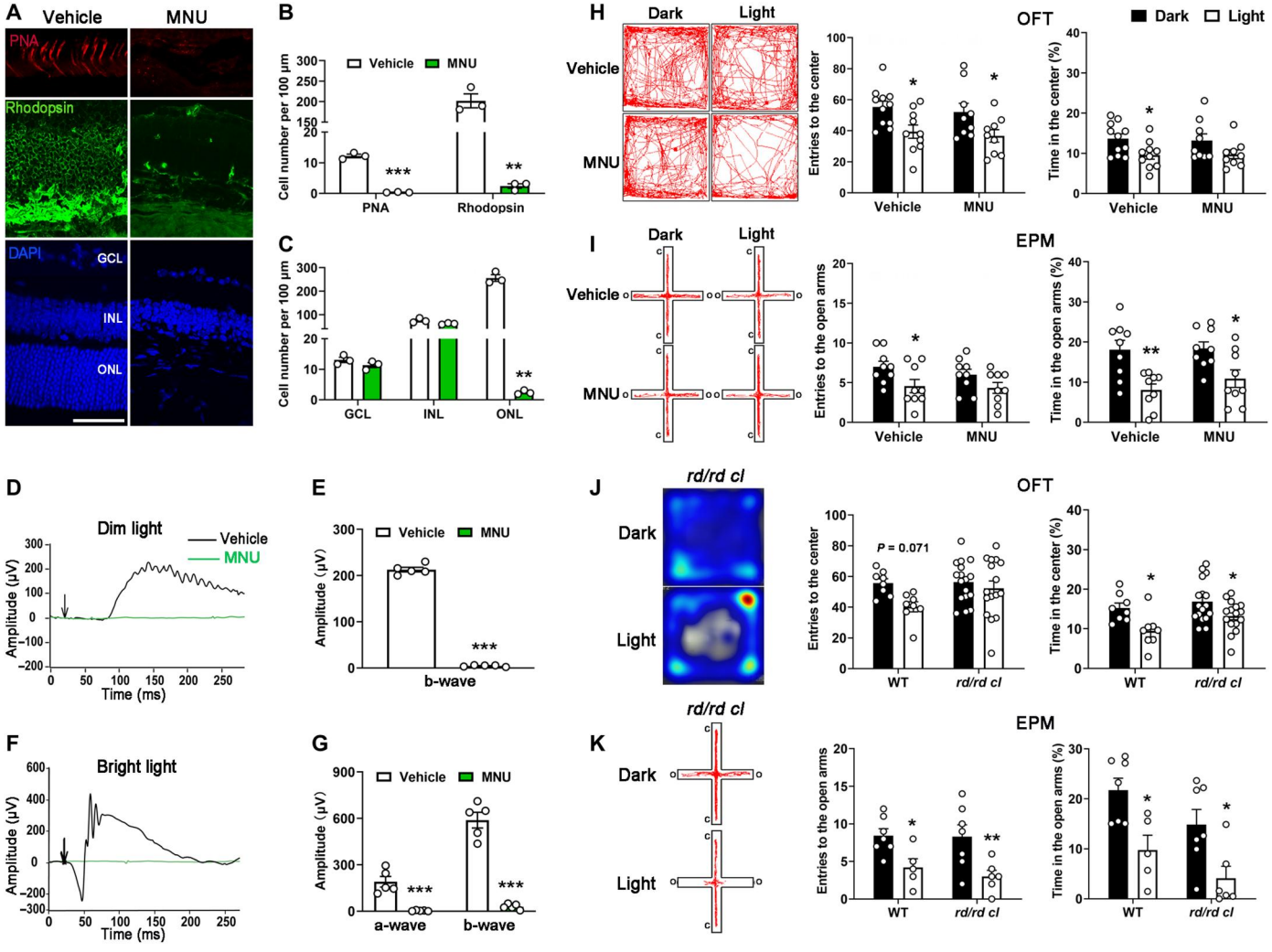

Fig. 2. The prolonged anxiogenic effect of light exposure is not dependent on rod/cone inputs. (**A**) Representative micrographs of retinal slices showing peanut agglutinin (PNA; cone marker, red), rhodopsin (rod marker, green), and DAPI (4′,6-diamidino-2-phenylindole; blue) staining captured from vehicle- and *N*-methyl-*N*-nitrosourea (MNU)–treated C57BL/6 mice. GCL, ganglion cell layer; INL, inner nuclear layer; ONL, outer nuclear layer. Scale bar, 50 μm. (**B** and **C**) Cell counts revealing that neurons positive for PNA/rhodopsin (B) and DAPI-stained nuclei in the ONL (C) were virtually missing after MNU treatment, whereas no apparent cell loss was observed in the GCL and INL. $^{**}P < 0.01$; $^{***}P < 0.001$, unpaired *t* test; $n = 3$ in each group. (**D** and **F**) Representative dark-adapted electroretinographic (ERG) recordings from mice with vehicle or MNU injections. Electroretinograms were evoked by dim [0.007 cd·s/m^2 (D)] and bright [4 cd·s/m^2 (F)] flashes (3 ms, arrows). (**E** and **G**) Compared to those in vehicle-injected animals, amplitudes of b-waves elicited by dim flashes (E) and a-/b-waves elicited by bright flashes (G) were all tremendously reduced in MNU-treated mice. $^{***}P < 0.001$, unpaired *t* test; $n = 5$ in each group. (**H** and **I**) Representative tracks (left) and pooled data (right) illustrating the effect of previous light pulse application (1000 lux, 25 min) on anxiety-like behaviors, as assessed by the OFT (H) and EPM (I), in vehicle- and MNU-treated animals. $^{*}P < 0.05$; $^{**}P < 0.01$, Sidak's multiple comparisons test; $n = 9$ to 11 in each group. (**J** and **K**) Representative tracks/heat maps (left) and pooled data (right) obtained from the OFT (J) and EPM (K) showing that the light-induced anxiety-like behaviors were largely preserved in *rd/rd cl* mice, which lack rods and cones. $^{*}P < 0.05$; $^{**}P < 0.01$, Sidak's multiple comparisons test; $n = 5$ to 17 in each group. All bar charts depict the means ± SEM. WT, wild type.

hematoxylin and eosin histological staining of the whole eyecup confirmed that the vast majority of these photoreceptors were ablated, and such ablation seems consistent along the entire length of the retina (fig. S5).

In line with this, electroretinographic (ERG) responses recorded in dark-adapted MNU-treated mice underwent great changes. As shown in Fig. 2 (D to G), both the b-waves ($P < 0.001$) evoked by dim flashes (0.007 cd·s/m^2 for rod-dominant responses) and the a- and b-waves (both $P < 0.001$) evoked by bright flashes (4 cd·s/m^2 for mixed rod/cone responses) were virtually abolished in MNU-treated animals, indicating the dysfunction of rod/cone photoreceptors. In addition, multielectrode array (MEA) recording demonstrated that light stimuli at intensities lower than the melanopsin activation threshold virtually failed to induce photoresponses in any channels in MNU-treated retinal whole mounts (fig. S6, A and B), suggesting that, although there might be a few residual rod/cone photoreceptors spared by MNU, they were unlikely to be functional.

Meanwhile, the gross morphology and the cell density in the inner retina, revealed by DAPI (4e,6-diamidino-2-phenylindole)

staining, were similar between the vehicle- and MNU-treated mice [$P > 0.05$ for both the ganglion cell layer (GCL) and the inner nuclear layer (INL); Fig. 2, A and C], although there appeared to be a tendency of reduced soma densities. Moreover, cells positive for melanopsin (ipRGC marker) and Brn3a (conventional RGC marker) in the GCL were both comparable between the two groups (both $P > 0.05$; fig. S7). Consistently, the "intrinsic" (rod/cone-independent) melanopsin-driven photoresponses of ipRGCs, isolated by a glutamatergic cocktail, remained normal in MNU group (fig. S6, C and D). These results indicated that MNU caused rapid apoptosis of the vast majority of rod/cone photoreceptors with high specificity.

When challenged with the OFT and EPM at 1 to 2 weeks after MNU injection, the results obtained in MNU-injected animals were largely similar to those obtained in vehicle-injected control animals (Fig. 2, H and I, and figs. S1B and S8A). That is, after light exposure, both the number of entries to the center (OFT, $P = 0.049$) and the time spent in the open arms (EPM, $P = 0.020$) were significantly reduced. A significantly increased thigmotaxis was also observed ($P = 0.042$). The time in the center (OFT, $P = 0.145$) and number of entries to the open arms (EPM, $P = 0.217$) of MNU-light group both showed a declining tendency, although the effect was not significant. The total distance traveled was not changed by the light exposure ($P = 0.075$).

A small fraction of rod/cone photoreceptors might survive the MNU treatment. Although the results of MEA recording argue for the dysfunction of these residual cells, MEAs only record a specific region of the retina and could miss areas of healthy surviving photoreceptors. Therefore, to confirm the minor role of the rod/cone photoreceptors in light-induced anxiety-like behaviors, *rd/rd cl* mice, which undergo rod/cone degeneration (*34*, *35*), were subjected to behavioral tests after light pulse application (Fig. 2, J and K, and figs. S1C and S8B). Similar to MNU-treated animals, *rd/rd cl* mice exhibited apparent light-induced anxiety-like behaviors, as suggested by reduced time spent in the center ($P = 0.042$) and increased thigmotaxis ($P = 0.0003$) in the OFT as well as reduced number of entries to and time spent in the open arms in the EPM ($P = 0.009$ and 0.020, respectively) after light exposure, although the number of entries to the center was not significantly changed in the OFT ($P = 0.667$). The total distance traveled was not significantly affected ($P = 0.840$). Together, we conclude that the prolonged light-induced anxiety-like behaviors can be produced almost independent of rod/cone inputs.

Melanopsin-driven ipRGC activities are indispensable for light-induced anxiety-like behaviors

To test the role of melanopsin, the newly identified nonrod, noncone photosensitive opsin (*36*), in the anxiogenic effect observed, $Opn4^{-/-}$ mice (*37*) and their wild-type (WT) littermates were challenged with the OFT and EPM (Fig. 3, A to C, and figs. S1D and S8C) after light pulse treatment. In contrast to the WTs, the experiments conducted in $Opn4^{-/-}$ mice showed that the number of entries to ($P = 0.240$) and time spent in the center ($P = 0.571$) in the OFT, as well as the thigmotactic behaviors ($P = 0.126$), were hardly changed, in addition to unchanged number of entries to and time spent in the open arms in the EPM ($P = 0.834$ and 0.357, respectively) after light pulse treatment. Meanwhile, the total distance traveled was also unaffected by the light exposure ($P = 0.877$). These results suggest that melanopsin-based phototransduction mediates the anxiety-like behaviors.

Melanopsin is predominantly expressed in ipRGCs. It was reasonable to speculate that ipRGCs may be the major retinal conduits for generating the anxiety-like behaviors that require melanopsin. To confirm the speculation, we conducted behavioral tests on ipRGC-ablated C57BL/6 mice. Selective ablation of ipRGCs was achieved by intravitreal injection of the immunotoxin melanopsin-saporin (SAP) (*12*). As shown in Fig. 3D, cell counting revealed that a single injection of 100 ng of SAP reduced the melanopsin-positive cell number by ~90% at 21 days after injection ($P < 0.001$). By contrast, the single injection of 100 ng of SAP did not affect the densities of conventional RGCs, cones, or rods (fig. S9, A to D) or did it significantly alter gross retinal structure or DAPI-stained nucleus densities in the outer nuclear layer (ONL), INL, and GCL (fig. S9, E and F). Furthermore, neither the b-wave ($P = 0.625$) evoked by dim flashes nor a- ($P = 0.877$) and b-waves ($P = 0.973$) evoked by bright flashes were significantly changed by the SAP injection (fig. S9, G to K), suggesting largely unchanged overall retinal function. In addition, in $Opn4^{Cre/+}$; *Ai14* mice, in which all melanopsin-expressing cells are labeled by tdTomato fluorescence (*38*), SAP did not cause appreciable changes in tdTomato-positive fibers within the cornea, arguing against a collateral damage of non-retinal ocular tissues (fig. S10). Thus, the SAP-induced ablation was highly specific to ipRGCs.

The OFT and EPM tests run on SAP-injected animals at 21 days after injection demonstrated that no significant changes were detected in all the parameters analyzed after light pulse application (OFT, $P = 0.954$ for center entries, $P = 0.543$ for center time, $P = 0.613$ for total distance, and $P = 0.113$ for thigmotaxis; EPM, $P = 0.999$ for open entries and $P = 0.974$ for open time), quite comparable with those obtained from $Opn4^{-/-}$ mice (Fig. 3, E and F, figs. S1E and S8D), suggesting that light-induced anxiety-like behaviors were absent in ipRGC-ablated C57BL/6 mice.

ipRGC-CeA circuit mediates light-induced anxiety-like behaviors

To determine the potential brain areas that may be associated with the light-induced anxiety-like behaviors, we first examined the effects of light exposure (1000 lux, 25 min) on the overall activity of different brain areas. To reflect the overall activity of an activity-associated nucleus, the expression levels of the immediate early gene c-*fos*, as represented by the number of neurons immuno-positive for its protein product c-Fos, were quantified (Fig. 4, A and B). As expected, in the suprachiasmatic nucleus (SCN), a brain nucleus receiving intense ipRGC projection, c-Foslevels were significantly higher in mice in light group than those in dark group ($P = 0.002$). In addition, significant bilateral c-Fos induction was detected in a battery of ipRGC-projected areas known to be involved in anxiety (*2*, *39*), such as the ventral lateral geniculate nucleus/intergeniculate leaflet (vLGN/IGL) ($P = 0.001$), CeA ($P = 0.027$), and BNST ($P = 0.036$). By contrast, c-Fos-positive cell numbers in the dorsal raphe nuclei (DRN), an anxiety-associated region lacking ipRGC projections (*40*), were comparable between light and dark groups ($P = 0.796$), disputing against its role in the observed anxiogenic effect.

Whether vLGN/IGL, CeA, and BNST are responsible for the light-induced anxiety-like behaviors was tested by inactivating neurons in these regions in a nonselective manner using an

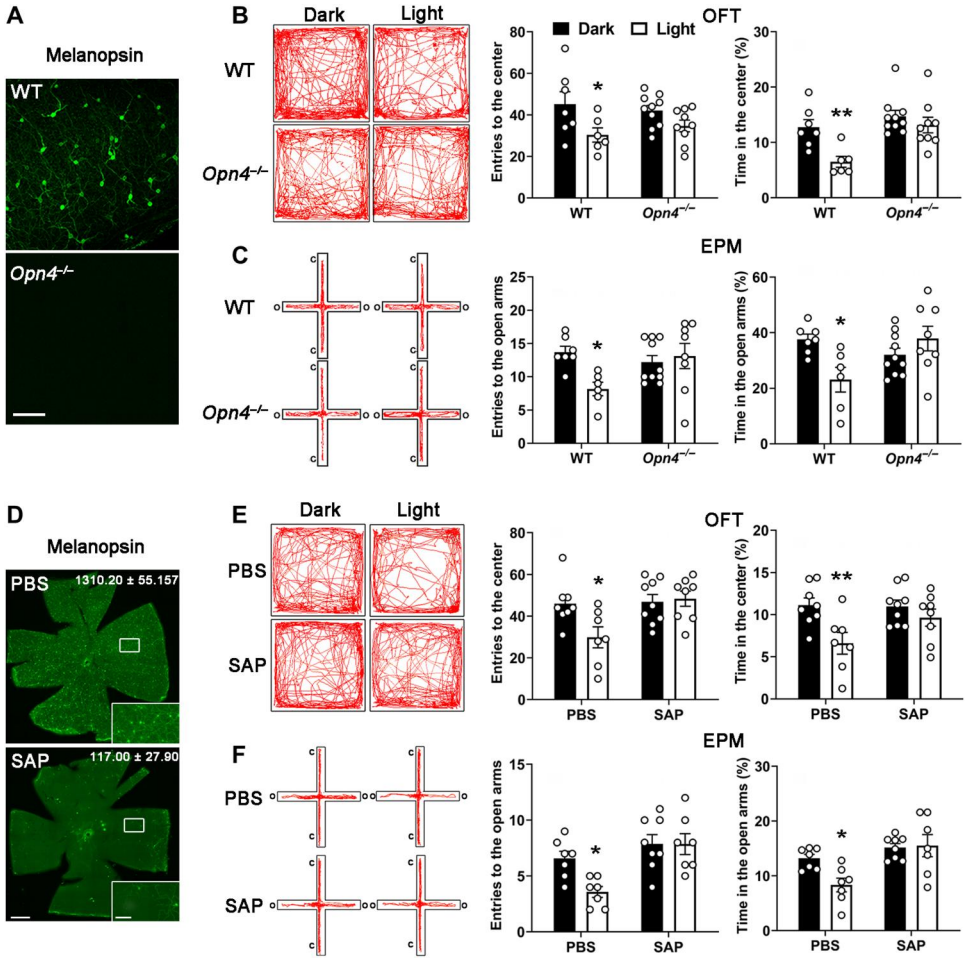

Fig. 3. Both melanopsin knockout and ipRGC ablation eliminate light-induced anxiety-like behaviors. (**A**) Melanopsin-immunoreactive signals were completely absent in an *Opn4*$^{-/-}$ retina (bottom), whereas a mosaic of melanopsin-positive cells was observed in the retina of a WT littermate (top). Scale bar, 100 μm. (**B** and **C**) Representative tracks (left) and pooled data (right) showing that unlike their WT littermates, *Opn4*$^{-/-}$ mice did not exhibit reduced number of entries to/time spent in the center [OFT (B)] and open arm [EPM (C)] after light pulse treatment (1000 lux, 25 min). **P* < 0.05; ***P* < 0.01, Sidak's multiple comparisons test; *n* = 6 to 10 in each group. (**D**) Microscopic images of retinal whole mounts stained with the melanopsin antibody, which were harvested from C57BL/6 mice injected with phosphate-buffered saline (PBS; top) or 100 ng of melanopsin-saporin (SAP; bottom). The boxed regions are enlarged and shown in the insets. Average numbers of melanopsin-positive cells per retina are listed in each panel. Scale bars, 500 μm in bottom panel and 100 μm in its inset. (**E** and **F**) Representative tracks (left) and pooled data (right) of the OFT (E) and EPM (F) illustrating the loss of the light-induced (1000-lux, 25-min) anxiety-like behaviors in SAP-injected animals. **P* < 0.05; ***P* < 0.01, Sidak's multiple comparisons test; *n* = 7 to 9 in each group. All values are expressed as the means ± SEM.

adeno-associated virus (AAV) expressing the enhanced green fluorescent protein (EGFP)–tagged chemogenetic inhibitor hM4Di (AAV-hSyn-hM4Di-EGFP). hM4Di was activated by intraperitoneal injection of clozapine *N*-oxide (CNO) at 3 weeks after viral delivery. However, for both the vLGN/IGL and BNST, which are innervated by ipRGCs (*28*), such chemogenetic manipulation resulted in significantly increased (~30%) baseline anxiety levels in darkness as revealed by the OFT (fig. S11), which would make it quite complicated to explain any data obtained with light pulse treatment. Thus, we chose not to conduct any further experiments on these two nuclei.

A previous anterograde tracing study revealed sparse ipRGC axons innervating the CeA (*27*). In this study, stereotaxic delivery of CTB-488 into the CeA of *Opn4*$^{Cre/+}$; *Ai14* mice, in which ipRGCs are labeled by tdTomato fluorescence, showed that the vast majority (78.20%) of retrogradely stained RGCs were positive for tdTomato, verifying a direct CeA-ipRGC input (Fig. 4, C and D). In C57BL/6 mice, hM4Di/CNO treatment of the CeA led to a significant decline in light-induced c-Fos expression in the CeA, confirming effective neuronal inhibition ($P = 0.009$; Fig. 4, E and F).

Effects of hM4Di/CNO-mediated CeA inhibition on anxiety-like behaviors were further examined (Fig. 4, G and H). CeA inhibition did not change the basal anxiety-like responses in darkness. However, unlike those observed in hM4Di/saline-treated control mice, it was found that in hM4Di/CNO-treated animals, none of the behavioral parameters of the OFT and EPM obtained in light group were significantly different from those obtained in dark group (OFT, $P = 0.586$ for center entries and $P = 0.859$ for center time; EPM, $P = 0.561$ for open entries and $P = 0.757$ for open time). Thus, CeA activation seems to be indispensable for light-induced anxiety-like behaviors.

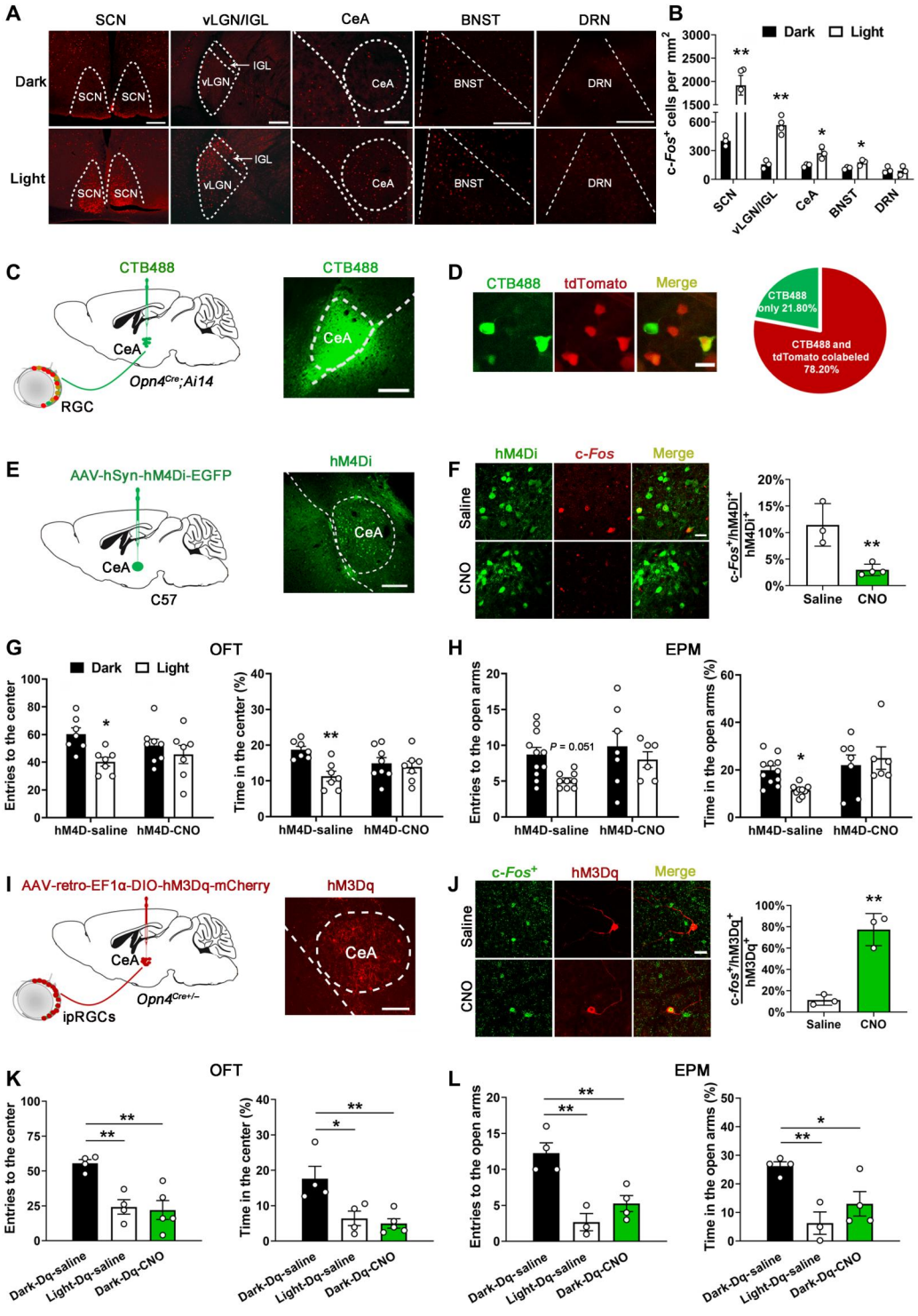

Fig. 4. The ipRGC-CeA projection is involved in the light-induced anxiogenic effects. (**A**) Representative micrographs showing c-Fos labeling in different brain regions in C57BL/6 mice treated with darkness or 1000-lux, 25-min light pulse. (**B**) Light treatment caused c-Fos induction in multiple brain nuclei including the central amygdala (CeA). $n = 3$ to 4. (**C**) Schematic and micrograph showing stereotaxic delivery of CTB-488 to the CeA and injection site in *Opn4*$^{Cre/+}$; *Ai14* mice. (**D**) Representative images and pie chart illustrating that most of CTB-488–retrolabeled retinal ganglion cells (RGCs) exhibited tdTomato fluorescence. $n = 4$ retinas; in each retina, 78 ± 6 CTB-488–positive RGCs were found. (**E**) Schematic of delivery of hM4Di-EGFP (enhanced green fluorescent protein) to the CeA of C57BL/6 mice and representative image showing the injection site. (**F**) Representative photomicrographs and grouped data showing reduced light-evoked c-Fos expression in the CeA in hM4Di/clozapine *N*-oxide (CNO)–treated mice. $n = 892$ cells (three mice) for saline and 1430 cells (four mice) for CNO. (**G** and **H**) Chemogenetic inhibition of CeA neurons eliminated the light-induced anxiety-like behaviors in C57BL/6 mice. $n = 6$ to 11. (**I**) Diagram of stereotaxic delivery of a Cre-inducible retrograde hM3Dq-mCherry virus to the CeA in *Opn4*$^{Cre/+}$ mice and representative image of the injection site. (**J**) Representative images and pooled data showing that CNO application increased the c-Fos expression in hM3Dq-mCherry–infected, CeA-projecting intrinsically photosensitive RGCs (ipRGCs) in *Opn4*$^{Cre/+}$ mice. $n = 72$ cells (three retinas) for saline and 62 cells (three retinas) for CNO. (**K** and **L**) Chemogenetic activation of CeA-projecting ipRGCs induced anxiety-like behaviors in darkness, which mimicked the light-induced anxiety-like behaviors. $n = 3$ to 5. Data are the means ± SEM. $^*P < 0.05$; $^{**}P < 0.01$; unpaired *t* test in (B), (F), and (J); Sidak's multiple comparisons test in (G) and (H); least significant difference (LSD) multiple comparisons test in (K) and (L). Scale bars, 200 μm in (A), (C), (E), and (I) and 20 μm in (D), (F), and (J).

We further tried to determine whether activation of the ipRGC-CeA circuit causes anxiogenic effects. For targetedly activating this circuit, we injected a retrograde AAV (AAV-retro-EF1α-DIO-hM3Dq-mCherry) encoding the mCherry-tagged hM3Dq chemogenetic activator in a Cre-dependent manner into the CeA of *Opn4*$^{Cre/+}$ mice (Fig. 4I). After 3 weeks, hM3Dq was found to be selectively expressed by CeA-projecting ipRGCs, and intraperitoneal CNO administration resulted in c-Fos induction in these cells in darkness (Fig. 4J), verifying that hM3Dq/CNO treatment could activate the ipRGC-CeA circuit.

In darkness, hM3Dq/CNO-treated *Opn4*$^{Cre/+}$ mice were challenged with behavioral tests at 60 min after CNO injection. They exhibited increased anxiety-like phenotypes in both the OFT ($P = 0.004$ for center entries and $P = 0.008$ for center time;

Fig. 4K) and EPM ($P = 0.009$ for open entries and $P = 0.048$ for open time; Fig. 4L), as compared to saline-injected controls, and such effects were generally comparable to the anxiogenic effects observed in hM3Dq/saline-treated animals with light pulse application. Meanwhile, when the CeA of *Opn4*$^{Cre/+}$ mice was injected with the nonactive viral construct (AAV2-retro-DIO-mCherry), CNO failed to induce any appreciable anxiety-like behaviors, thus arguing against a direct, hM3Dq-independent contribution of CNO (fig. S12). All these results provide further evidence that the ipRGC-CeA innervation dominantly mediates light-induced anxiety-like behaviors.

The role of CORT system

Whether the anxiogenic effect may be accompanied by elevated levels of CORT release and GR expression, which have been shown to mediate anxiety-like symptoms (*41*–*43*), was investigated. First, enzyme-linked immunosorbent assay (ELISA) showed that neither the serum ($P = 0.637$) nor the cerebrospinal fluid (CSF) ($P = 0.475$) CORT levels were significantly changed after light pulse treatment (Fig. 5, A and B). However, quantitative Western blot analysis, conducted on samples harvested from various brain regions, revealed that the protein levels of GRs in the CeA and BNST were both significantly increased ($P = 0.043$ for CeA and $P = 0.011$ for BNST; Fig. 5, C and D). Meanwhile, light pulse application promoted the phosphorylation of GRs in both the CeA and BNST ($P = 0.035$ for CeA and $P = 0.004$ for BNST; Fig. 5, C and E). Moreover, subcutaneous injection of the specific GR antagonist RU486 (100 mg/kg) (Fig. 5, F and G) completely eliminated the light-induced anxiety-like behaviors, as shown by highly comparable parameters yielded by the OFT ($P = 1.000$ for center entries and $P = 0.426$ for center time) and EPM ($P = 0.994$ for open entries and $P = 0.427$ for open time) between light and dark groups.

DISCUSSION

In this study, we uncovered that short-term bright light exposure induces prolonged anxiety-like behaviors, which are mainly mediated by melanopsin-driven ipRGC activity. Because the two genetically deficient mice, *rd/rd cl* and *Opn4*$^{-/-}$, might have developmental reorganization of visual circuits that add to the difficulty of data explanation, the same behavioral experiments were also conducted on adult WT C57BL/6 mice with MNU/SAP treatment. Highly comparable results from both genetically and pharmacologically manipulated mice were obtained.

The anxiety-like behaviors could only be induced by high-intensity light, but were notably persistent, lasting for a period even longer than the light exposure. These features may be derived from the well-documented characteristics of melanopsin-mediated photoresponses with rather higher light threshold and long-lasting time course (*32*, *44*), although the prolonged characteristic could also be ascribed to certain biochemical effects, such as those mediated by CORT. It is of interest that some other NIF visual functions requiring persistent light, such as light aversion (*45*), sustained phase of the pupillary light reflex (*46*), and maintenance of light-induced sleep (*47*), are invariably associated with melanopsin signals.

Six subtypes of ipRGCs with distinct structural-functional profiles have been characterized in mice (*48*, *49*). The exact ipRGC subtype(s) mediating the anxiogenic effect observed in this study have yet to be determined. The anxiety-like responses seen in the chemogenetically manipulated dark group *Opn4*$^{Cre/+}$ mice (Fig. 4, I to L) could be due to the activation of any of subtypes, considering that hM3Dq (G_q)–mediated activation of ipRGCs in these mice seems not to bias toward a specific subtype (*29*, *50*). Meanwhile, the results that anxiety-like behaviors were eliminated by SAP treatment suggests a possibility that they may be caused by the activation of M1 to M3 subtypes, because this immunotoxin is made on the basis of the antibody preferentially targeting these three subtypes with relatively higher melanopsin expression (*51*, *52*). Transgenic mice (*53*, *54*) and genetic tools (*16*) that enable the manipulation of specific ipRGC subtypes could be used to resolve this issue. However, M1s are primarily driven by melanopsin phototransduction, whereas the photoresponses of M2s and M3s are mainly mediated by rod/cone inputs (*55*). Given that loss of melanopsin alone can abolish the light-induced anxiogenic effect, it is reasonable to consider that M1s are the key ipRGC subtype for the anxiogenic effect that we observed, although the involvement of M2s and/or M3s is also possible. On the other hand, it may be that central neurons are able to distinguish melanopsin signals from rod/cone signals, both routed via ipRGCs, based on their distinct photosensitivity, spectral sensitivity, response dynamics, etc. (*46*). For instance, a recent study shows that melanopsin signals specifically modulate ocular axial changes during eye growth, while rod/cone signals of ipRGCs mainly contribute to the corneal development (*56*).

Note that in MNU-treated animals, the time in the center (OFT) and number of entries to the open arms (EPM) of light group were not statistically distinct from those of dark group (Fig. 2, H and I). Similarly, the number of entries to the center (OFT) was not changed by light exposure in *rd/rd cl* mice (Fig. 2J). Although these results might simply reflect variability across tests, they could also be attributable to a relatively minor influence of rod/cone photoreceptors. Meanwhile, ~20% of CeA-projecting RGCs were found to be tdTomato-negative in *Opn4*$^{Cre/+}$*; Ai14* mice (Fig. 4D). These cells are very likely to be conventional RGCs and might constitute another, although less important, retinal conduit for the light-induced anxiety-like behaviors.

Our data shown in Fig. 4 (G and H), in particular, the result showing almost complete suppression of the light-induced anxiety-like behaviors, by hM4Di/CNO-elicited chemogenetic inhibition of CeA, demonstrated a critical role of this brain area in this anxiogenic effect. It should be emphasized that the involvement of other ipRGC-innervated areas related to anxiety, such as the BNST and vLGN, could not be ruled out. It is known that there are complex interactions between the CeA and other brain regions (*2*, *57*). Moreover, because ipRGCs have diverse targets (*26*–*28*, *58*), chemogenetic activation of CeA-projecting ipRGCs might lead to the activation of other regions regulating anxiety levels. Notably, the master circadian pacemaker SCN, one of the primary targets of ipRGCs that exhibits high c-Fos expression in response to our light exposure paradigm (Fig. 4, A and B), is recently found to regulate anxiety-related behaviors in mice (*59*). In addition, circadian expression of PER2 protein in the CeA is reportedly controlled by inputs from the SCN together with hormonal/neurochemical circadian alterations (*60*). Therefore, the ipRGC–SCN circuit might be another, circadian rhythm-based, mechanism underlying the light-induced anxiogenic effect observed in this study, either in a

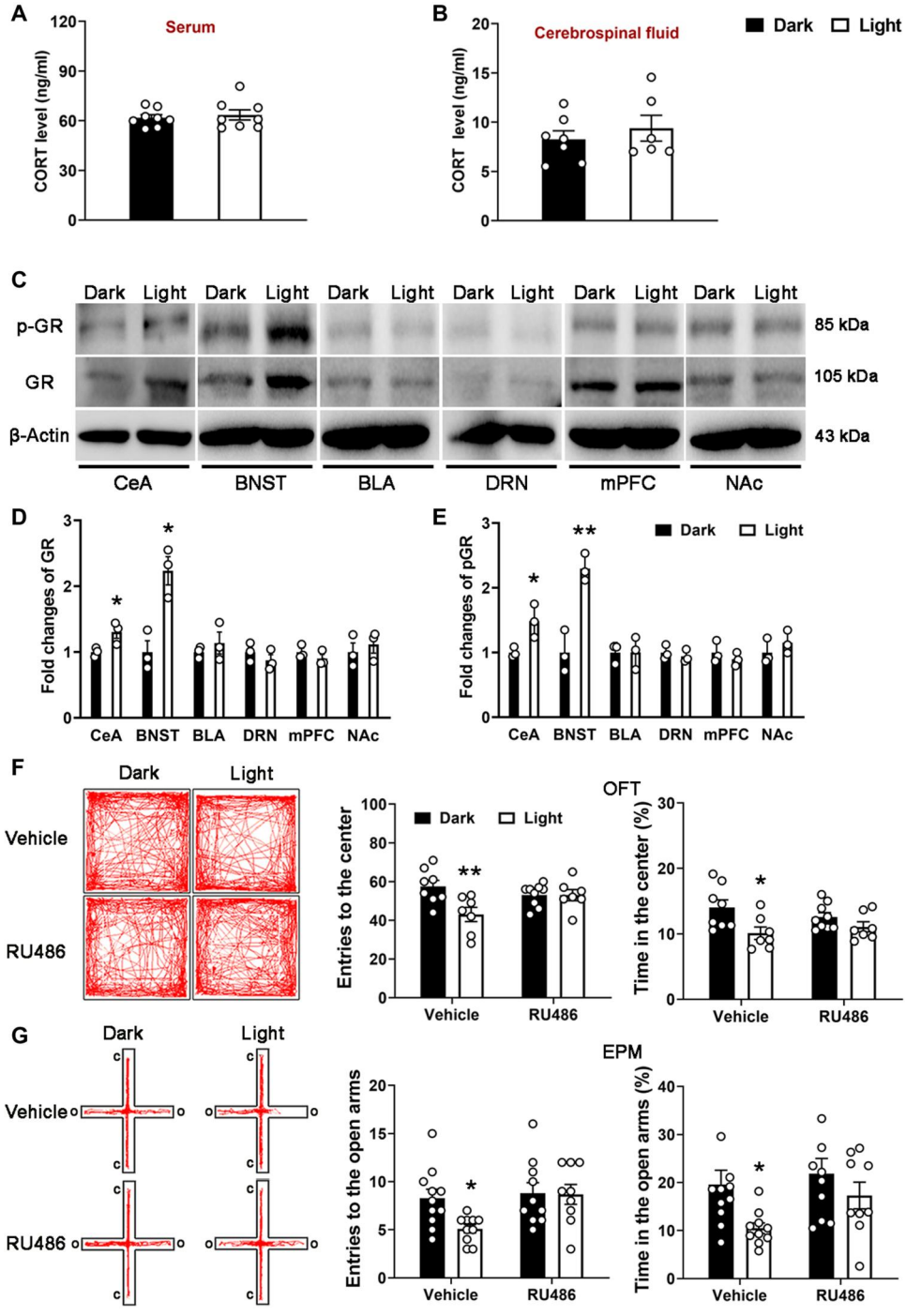

Fig. 5. Blocking the action of glucocorticoids eliminates light-induced anxiety-like behaviors. (**A** and **B**) Bart charts showing that neither the serum (A) nor CSF (B) corticosterone (CORT) levels were altered following the 1000-lux, 25-min light pulse treatment in C57BL/6 mice. Unpaired *t* test, $n = 6$ to 8 in each group. (**C** to **E**) Representative photographs of Western blots (C) and pooled data (D and E) showing a significant increase in protein levels of glucocorticoid receptor (GR) and its phosphoisoform (p-GR) in the CeA, bed nucleus of the stria terminalis (BNST), basolateral amygdala (BLA), dorsal raphe nuclei (DRN), medial prefrontal cortex (mPFC), and nucleus accumbens (NAc) of light pulse–treated animals. $^{*}P < 0.05$; $^{**}P < 0.01$, unpaired *t* test; $n = 3$ in each group. (**F** and **G**) Representative tracks (left) and pooled data (right) showing that C57BL/6 mice injected with RU486, a GR antagonist, no longer exhibited reduced number of entries to/time spent in the center [OFT (F)] and open arm [EPM (G)] after light pulse treatment. $^{*}P < 0.05$; $^{**}P < 0.01$, Sidak's multiple comparisons test; $n = 7$ to 11 in each group. All bar charts depict the means ± SEM.

separate or a synergistic manner. More exquisite approaches could shed more light on this issue.

Although ELISA showed that neither the serum nor the CSF CORT levels changed significantly, the protein levels of GRs and phosphorylation of GRs in the CeA and BNST were significantly increased after light pulse exposure, strongly suggesting the possible involvement of the CORT system. This possibility was further strengthened by the result showing a complete elimination of the prolonged anxiogenic effect by subcutaneous injection of the specific GR antagonist RU486. While previous studies revealed fast GR expression in various regions in the CNS (*61*, *62*), the mechanisms underlying the observed rapid GR-level increment and how it could account for the anxiogenic effect remain to be further explored. The activities mediated by CORT, a stress hormone, may last for a long period of time (*63*, *64*), thus being responsible for the post-effect of light, as observed in this study.

From an evolutionary perspective, anxiety serves as an adaptive function, prompting an animal to evaluate the confronting threats and respond in an appropriate and timely manner (*65*). For the mouse, a nocturnal animal, abrupt exposure to bright light would invariably indicate a situation of incoming danger, such as loss of shelter and emergence of fire. In some circumstances, temporary disappearance of the signs of danger does not necessarily mean the complete extinction of it. In this context, an appropriately "delayed" removal of anxiety status, just like the postexposure anxiogenic effects observed in this study, is likely to further minimize attacks from temporally invisible threats, conferring a survival advantage.

It is of interest that light pulse exposure did not modulate depressive-like behaviors, another class of mood-relevant effects closely associated with anxiety-like behaviors, although both chronic and acute light at night provokes depressive-like phenotypes (*24*, *66*–*69*). The results yielded by the tail suspension test (TST) and forced swimming test (FST), two standard behavioral paradigms for evaluating depressive-like behaviors, in an independent cohort of C57BL/6 mice (fig. S13) revealed that immobile durations in the TST ($P = 0.697$) and FST ($P = 0.581$) in 1000-lux light pulse-treated mice were not significantly different from those of dark group. The immobile durations of the TST and FST were hardly changed even following a 3000-lux light pulse ($P = 0.903$ for TST and $P = 0.743$ for FST).

It has been shown that brief light exposure to nocturnal animals acutely induces locomotor suppression and sleep (*70*). This seems at odds with the increased anxiety-like responses (generally thought to be linked to enhanced arousal rather than sleep) that we observed in light pulse–treated mice. Even during the 25-min light application period, no evident signs of sleep-promoting effects were observed; instead, increased arousal/anxiety was seen, consistent with the results of two recent studies (*9*, *29*). This may be accounted for by the fact that we chose to apply the light exposure during the nocturnal active period (ZT14 to ZT17) of mice with low homeostatic sleep pressure. In addition, it could be explained by the recently identified, intricate role of light in regulating mouse sleep: Blue light (470 nm) causes behavioral arousal, whereas green light (530 nm) produces sleep induction (*17*). The light pulse used in this study was provided by a 6500-K light source, the emission spectrum of which contains more "blue" components than "green" ones; therefore, the overall effect was arousal/alertness promoting but not sleep inducing.

Whether the results obtained in mice in this study could be readily applicable to diurnal humans awaits further study. However, acute light exposure has direct impacts on alertness and electroencephalogram in humans (*71*). Bright light exposure could also represent potential threats (e.g., fire and weather changes) to humans. Therefore, it is likely that the human nervous system has also developed a mechanism controlling an analog of the mouse light-induced anxiety-like behaviors during evolution. Given the increasing application of artificial lighting in the human environment, such a mechanism might result in "unnecessary" anxiety, leading to pathological conditions. Our findings might inspire future studies focusing on the mechanisms and intervention strategies for pathological postlight effects in human patients.

MATERIALS AND METHODS

Animals

Adult (>6 weeks) C57BL/6, melanopsin knockout ($Opn4^{-/-}$) (*37*), $Opn4^{Cre/+}$; *Ai14* [a cross of $Opn4^{Cre/+}$ (*72*) and Ai14 reporter line] and rodless-coneless (*rd/rd cl*) mice [generated by crossing the *rd1* mouse, which has a PDE6b variant causing rod degeneration, with the *Cone-DTA* mouse, which has an additional allele driving diphtheria toxin A (DTA) expression under the human cone opsin promoter to ablate cones] (*34*, *35*) were used in this study. For experiments using knockout/mutant animals, WT littermates were used as controls. All animal procedures were approved by the Fudan University Institutional Animal Care and Use Committee.

Behavioral tests

Before experiments, mice were housed in a timer-controlled 12-hour light/12-hour dark (LD) cycle (lights on at 7:00 a.m., ~150-lux white ambient illumination) for at least 14 days. The mice were then kept in the dark (DD) for 26 to 29 hours. The dark adaptation always started at ZT12, and the light stimulation and behavioral tests were conducted between ZT14 and ZT17 of the next day. Because the time in DD was short (<29 hours) and the free running period of mice is known to be close to 24 hours [~23.3 hours in C57 mice (*73*)], the circadian time (CT) at the time of light stimulation approximately equals to the ZT in the previous LD cycle, i.e., CT = ZT. Therefore, actually, for all mice, light exposure was invariably applied in the early dark phase (approximately CT14 to CT17). Full-spectrum light pulses were generated by an array of light-emitting diode (LED) lamps (6500 K; Philips, Netherlands). In a pilot experiment, we used a light pulse (1000-lux) series with ascending durations (10, 20, 25, 30 min, etc.), trying to determine the most "appropriate" light exposure duration. We found that a 10-min exposure only generated a small anxiogenic effect, and the effect of light exposure from 10 to 25 min was increased as a function of exposure time (fig. S14). However, when the exposure time was extended to 30 min or longer, sleep was induced in some of the animals tested, which would obviously perturb subsequent behavioral experiments. Therefore, we lastly decided to use 25 min throughout this study. After the 25-min light pulse application, animals were readapted to the dark for 1 min (for most experiments) or for 20, 60, and 120 min (for experiments examining the persistence of the postexposure anxiety-like behaviors) and then transferred to the testing device, after which the behavioral activities were recorded in darkness under far-red illumination. In the OFT,

mice were placed at the center of a square box (40 by 40 by 40 cm) and allowed to explore for 10 min. Time spent in and number of entries to the center area (24 by 24 cm), time spent close the walls (<2.5 cm), and the total distance travelled were recorded and analyzed by a computerized tracking system (EthoVision XT12, Noldus Information Technology, USA). In the EPM, mice were placed in the center of the maze (open arms: 30 by 5 cm, closed arms: 30 by 5 by 18 cm, and central platform: 5 by 5 cm) facing an open arm and allowed to freely explore the arena during the 5-min test session. Time spent in and number of entries to the open arms were measured with the EthoVision system.

ERG recording

Mice were dark-adapted overnight, then anesthetized (0.6% pentobarbital sodium, 12 μl/g ip), and moved into the Ganzfeld dome. ERG responses were recorded as previously described (*74*). Three-millisecond white light flashes (6000 K, 0.007 or 4 cd·s/m^2) were applied at 3-min intervals. Amplitudes of a-waves were measured from baseline, and amplitudes of b-waves were measured from the maximum negative to positive peaks of the recorded responses.

Intracranial injection and chemogenetic manipulation

Mice were anesthetized with pentobarbital sodium. Injections were performed stereotaxically using a microinjector (Nanoliter 2010, World Precision Instruments, USA). To specifically inhibit neurons in the BNST, vLGN/IGL, and CeA in C57BL/6 mice, rAAV2/9-hSyn-hM4Di-EYFP (2 to 4 × 10^{12} particles per ml; BrainVTA, China) was bilaterally injected (200 to 350 nl in each site). Because this virus is not Cre dependent and thus nonselectively inhibiting any neurons expressing it, the injection sites were checked carefully to make sure that no obvious off-target expression of hM4Di occurred during penetration and withdrawal of the microinjector. To selectively activate CeA-projecting ipRGCs, AAV2/retro-EF1α-DIO-hM3Dq-mCherry (1 × 10^{13} particles per ml; BrainVTA, China) was bilaterally injected into the CeA of *Opn4*$^{Cre/+}$ mice. On the day of the behavioral tests, mice were injected (intraperitoneally) with either saline or CNO (5 mg/kg; A3317, APExBIO, USA) 60 min before testing.

Enzyme linked immunosorbent assay

CSF samples were obtained as previously described (*75*). Briefly, the mouse was head-fixed at a 90° angle. A sharpened needle was used to penetrate the cisterna magna membrane to collect the CSF, which was transferred to a 0.6-ml microfuge tube, snap-frozen, and stored. Blood samples were harvested from the angular vein. After clot formation, the samples were centrifuged at 3000*g*, and the serum was obtained. CORT levels were measured from 1:10 diluted samples using an ELISA kit (R&D Systems, USA) according to the manufacturer's instructions.

Western blot analysis

Mice were euthanized at ~30 min after the termination of the light exposure; and the CeA, BNST, basolateral amygdala (BLA), DRN, medial prefrontal cortex (mPFC), and nucleus accumbens (NAc) were dissected and processed with a protein extraction kit (K268-50, BioVision, USA). Samples (50 μg per lane) were processed as previously described with the primary antibodies [rabbit anti-GR (1:500; A2164, ABclonal, China), rabbit anti–phospho-GR (1:500; AP0759, ABclonal, China), and mouse anti–β-actin (1:1000; Cell Signaling Technology, USA)] at 4°C for 24 hours. The membrane was incubated with horseradish peroxidase–conjugated secondary antibodies (1:5000; Cell Signaling Technology, USA) and processed with an enhanced chemiluminescence detection system (Amersham Pharmacia Biotech, USA).

Immunofluorescence

Mice were anesthetized and perfused intracardially with 0.9% saline, followed by 4% paraformaldehyde in phosphate buffer. Cone and rod photoreceptors were probed with PNA (1:500; RL-1072-5, Vector, USA) and a rhodopsin antibody (1:500; MAB5356, Chemicon, USA), respectively, in retinal sections (20 μm), while ipRGCs and conventional RGCs were stained with a melanopsin antibody [1:10000; AB-N38 (UF008), Advanced Targeting Systems, USA] and a Brn3a antibody (1:1000; 31984, Santa Cruz Biotechnology, USA), respectively, in retinal whole mounts. To quantify light-induced c-Fos expression, after the 25-min light exposure, mice were kept in DD for 90 min and then anesthetized and perfused. c-Fos signals were detected in brain slices (40 μm) or retinal whole mounts with a polyclonal antibody (1:1000; 226 004, Synaptic Systems, Germany). All Alexa Fluor dye–conjugated secondary antibodies were used at a dilution of 1:400.

MEA recording

Dark-adapted (>12 hour) mice were overdosed with 0.6% pentobarbital sodium. One eye was enucleated and transferred into Ames' medium equilibrated with 95% O_2 and 5% CO_2 under dim red light. The retina was dissected, mounted on a piece of Anodisc filter membrane (Whatman, USA), and transferred into the recording chamber of an MEA chip (60MEA200/30iR-ITO-gr, Multi Channel Systems, Germany) and then continuously superfused at 5 to 6 ml/min with Ames' medium. Voltage data were high-pass filtered at 200 Hz, digitized at 10 kHz, and amplified and acquired using the USB-MEA60-Inv-BC-System and MC_Rack Software (Multi Channel Systems). The retina was stimulated with full-field light flashes generated by an LED illuminator (Model 66991, DiCon Fiberoptics Inc., USA) and delivered onto the retina by a fiber optic cable. Wavelength and light intensity were adjusted by introducing narrowband interference filters and neutral density filters (Edmund Optics Inc., USA) into the light path. Melanopsin-based ipRGC responses were isolated with a glutamatergic blocker cocktail, which consisted of 50 μM L-AP4 (group III metabotropic glutamate receptor agonist; Tocris), 40 μM DNQX (AMPA/kainate receptor antagonist; Tocris), 30 μM D-AP5 (*N*-methyl-D-aspartate receptor antagonist, Tocris), and 2 μM ACET (kainate receptor antagonist, Tocris).

Statistical analyses

Comparisons between two independent groups were conducted with an unpaired *t* test. Comparisons among three groups were conducted with one-way analysis of variance (ANOVA), followed by least significant difference (LSD) post hoc comparisons. Two-way ANOVA was used to test for effects of light condition (light or dark), genotype/toxin/reagent or their interaction on anxiety-like behaviors (see data file S1 for detailed information). If a light, mutant/treatment, or interaction effect was detected, then post hoc Sidak's multiple comparisons test was used to determine differences between individual groups. $P < 0.05$ was considered statistically significant.

Supplementary Materials

This PDF file includes:
Figs. S1 to S14

Other Supplementary Material for this manuscript includes the following:
Data file S1

View/request a protocol for this paper from *Bio-protocol*.

REFERENCES AND NOTES

1. S. Fischer, The hypothalamus in anxiety disorders. *Handb. Clin. Neurol.* **180**, 149–160 (2021).
2. A. Adhikari, Distributed circuits underlying anxiety. *Front. Behav. Neurosci.* **8**, 112 (2014).
3. T. A. Bedrosian, R. J. Nelson, Timing of light exposure affects mood and brain circuits. *Transl. Psychiatry* **7**, e1017 (2017).
4. T. A. LeGates, D. C. Fernandez, S. Hattar, Light as a central modulator of circadian rhythms, sleep and affect. *Nat. Rev. Neurosci.* **15**, 443–454 (2014).
5. T. A. Bedrosian, R. J. Nelson, Influence of the modern light environment on mood. *Mol. Psychiatry* **18**, 751–757 (2013).
6. J. C. Borniger, Z. D. McHenry, B. A. Abi Salloum, R. J. Nelson, Exposure to dim light at night during early development increases adult anxiety-like responses. *Physiol. Behav.* **133**, 99–106 (2014).
7. T. Ikeno, S. P. Deats, J. Soler, J. S. Lonstein, L. Yan, Decreased daytime illumination leads to anxiety-like behaviors and HPA axis dysregulation in the diurnal grass rat (*Arvicanthis niloticus*). *Behav. Brain Res.* **300**, 77–84 (2016).
8. E. Roman, L. Arborelius, Male but not female Wistar rats show increased anxiety-like behaviour in response to bright light in the defensive withdrawal test. *Behav. Brain Res.* **202**, 303–307 (2009).
9. X. Huang, P. Huang, L. Huang, Z. Hu, X. Liu, J. Shen, Y. Xi, Y. Yang, Y. Fu, Q. Tao, S. Lin, A. Xu, F. Xu, T. Xue, K. F. So, H. Li, C. Ren, A visual circuit related to the nucleus reuniens for the spatial-memory-promoting effects of light treatment. *Neuron* **109**, 347–362.e7 (2021).
10. D. M. Berson, F. A. Dunn, M. Takao, Phototransduction by retinal ganglion cells that set the circadian clock. *Science* **295**, 1070–1073 (2002).
11. S. Hattar, H. W. Liao, M. Takao, D. M. Berson, K. W. Yau, Melanopsin-containing retinal ganglion cells: Architecture, projections, and intrinsic photosensitivity. *Science* **295**, 1065–1070 (2002).
12. D. Goz, K. Studholme, D. A. Lappi, M. D. Rollag, I. Provencio, L. P. Morin, Targeted destruction of photosensitive retinal ganglion cells with a saporin conjugate alters the effects of light on mouse circadian rhythms. *PLOS ONE* **3**, e3153 (2008).
13. A. D. Guler, J. L. Ecker, G. S. Lall, S. Haq, C. M. Altimus, H. W. Liao, A. R. Barnard, H. Cahill, T. C. Badea, H. Zhao, M. W. Hankins, D. M. Berson, R. J. Lucas, K. W. Yau, S. Hattar, Melanopsin cells are the principal conduits for rod-cone input to non-image-forming vision. *Nature* **453**, 102–105 (2008).
14. M. Hatori, H. Le, C. Vollmers, S. R. Keding, N. Tanaka, C. Schmedt, T. Jegla, S. Panda, Inducible ablation of melanopsin-expressing retinal ganglion cells reveals their central role in non-image forming visual responses. *PLOS ONE* **3**, e2451 (2008).
15. A. C. Rupp, M. Ren, C. M. Altimus, D. C. Fernandez, M. Richardson, F. Turek, S. Hattar, T. M. Schmidt, Distinct ipRGC subpopulations mediate light's acute and circadian effects on body temperature and sleep. *eLife* **8**, e44358 (2019).
16. Z. Zhang, C. Beier, T. Weil, S. Hattar, The retinal ipRGC-preoptic circuit mediates the acute effect of light on sleep. *Nat. Commun.* **12**, 5115 (2021).
17. V. Pilorz, S. K. Tam, S. Hughes, C. A. Pothecary, A. Jagannath, M. W. Hankins, D. M. Bannerman, S. L. Lightman, V. V. Vyazovskiy, P. M. Nolan, R. G. Foster, S. N. Peirson, Melanopsin regulates both sleep-promoting and arousal-promoting responses to light. *PLoS Biol.* **14**, e1002482 (2016).
18. J. W. Tsai, J. Hannibal, G. Hagiwara, D. Colas, E. Ruppert, N. F. Ruby, H. C. Heller, P. Franken, P. Bourgin, Melanopsin as a sleep modulator: Circadian gating of the direct effects of light on sleep and altered sleep homeostasis in Opn4(−/−) mice. *PLoS Biol.* **7**, e1000125 (2009).
19. D. Lupi, H. Oster, S. Thompson, R. G. Foster, The acute light-induction of sleep is mediated by OPN4-based photoreception. *Nat. Neurosci.* **11**, 1068–1073 (2008).
20. C. M. Altimus, A. D. Guler, K. L. Villa, D. S. McNeill, T. A. Legates, S. Hattar, Rods-cones and melanopsin detect light and dark to modulate sleep independent of image formation. *Proc. Natl. Acad. Sci. U.S.A.* **105**, 19998–20003 (2008).
21. D. C. Fernandez, P. M. Fogerson, L. Lazzerini Ospri, M. B. Thomsen, R. M. Layne, D. Severin, J. Zhan, J. H. Singer, A. Kirkwood, H. Zhao, D. M. Berson, S. Hattar, Light affects mood and learning through distinct retina-brain pathways. *Cell* **175**, 71–84.e18 (2018).
22. T. A. LeGates, C. M. Altimus, H. Wang, H. K. Lee, S. Yang, H. Zhao, A. Kirkwood, E. T. Weber, S. Hattar, Aberrant light directly impairs mood and learning through melanopsin-expressing neurons. *Nature* **491**, 594–598 (2012).
23. S. K. Tam, S. Hasan, S. Hughes, M. W. Hankins, R. G. Foster, D. M. Bannerman, S. N. Peirson, Modulation of recognition memory performance by light requires both melanopsin and classical photoreceptors. *Proc. Biol. Sci.* **283**, 20162275 (2016).
24. K. An, H. Zhao, Y. Miao, Q. Xu, Y. F. Li, Y. Q. Ma, Y. M. Shi, J. W. Shen, J. J. Meng, Y. G. Yao, Z. Zhang, J. T. Chen, J. Bao, M. Zhang, T. Xue, A circadian rhythm-gated subcortical pathway for nighttime-light-induced depressive-like behaviors in mice. *Nat. Neurosci.* **23**, 869–880 (2020).
25. L. Huang, Y. Xi, Y. Peng, Y. Yang, X. Huang, Y. Fu, Q. Tao, J. Xiao, T. Yuan, K. An, H. Zhao, M. Pu, F. Xu, T. Xue, M. Luo, K. F. So, C. Ren, A visual circuit related to habenula underlies the antidepressive effects of light therapy. *Neuron* **102**, 128–142.e8 (2019).
26. J. Y. Li, T. M. Schmidt, Divergent projection patterns of M1 ipRGC subtypes. *J. Comp. Neurol.* **526**, 2010–2018 (2018).
27. A. Delwig, D. D. Larsen, D. Yasumura, C. F. Yang, N. M. Shah, D. R. Copenhagen, Retinofugal projections from melanopsin-expressing retinal ganglion cells revealed by intraocular injections of Cre-dependent virus. *PLOS ONE* **11**, e0149501 (2016).
28. S. Hattar, M. Kumar, A. Park, P. Tong, J. Tung, K. W. Yau, D. M. Berson, Central projections of melanopsin-expressing retinal ganglion cells in the mouse. *J. Comp. Neurol.* **497**, 326–349 (2006).
29. N. Milosavljevic, J. Cehajic-Kapetanovic, C. A. Procyk, R. J. Lucas, Chemogenetic activation of melanopsin retinal ganglion cells induces signatures of arousal and/or anxiety in mice. *Curr. Biol.* **26**, 2358–2363 (2016).
30. M. Pant, A. J. Zele, B. Feigl, P. Adhikari, Light adaptation characteristics of melanopsin. *Vision Res.* **188**, 126–138 (2021).
31. D. M. Dacey, H. W. Liao, B. B. Peterson, F. R. Robinson, V. C. Smith, J. Pokorny, K. W. Yau, P. D. Gamlin, Melanopsin-expressing ganglion cells in primate retina signal colour and irradiance and project to the LGN. *Nature* **433**, 749–754 (2005).
32. K. Y. Wong, F. A. Dunn, D. M. Graham, D. M. Berson, Synaptic influences on rat ganglion-cell photoreceptors. *J. Physiol.* **582**, 279–296 (2007).
33. K. Yoshizawa, J. Yang, H. Senzaki, Y. Uemura, Y. Kiyozuka, N. Shikata, Y. Oishi, H. Miki, A. Tsubura, Caspase-3 inhibitor rescues *N*-methyl-*N*-nitrosourea-induced retinal degeneration in Sprague-Dawley rats. *Exp. Eye Res.* **71**, 629–635 (2000).
34. R. J. Lucas, M. S. Freedman, M. Munoz, J. M. Garcia-Fernandez, R. G. Foster, Regulation of the mammalian pineal by non-rod, non-cone, ocular photoreceptors. *Science* **284**, 505–507 (1999).
35. M. S. Freedman, R. J. Lucas, B. Soni, M. von Schantz, M. Munoz, Z. David-Gray, R. Foster, Regulation of mammalian circadian behavior by non-rod, non-cone, ocular photoreceptors. *Science* **284**, 502–504 (1999).
36. X. Qiu, T. Kumbalasiri, S. M. Carlson, K. Y. Wong, V. Krishna, I. Provencio, D. M. Berson, Induction of photosensitivity by heterologous expression of melanopsin. *Nature* **433**, 745–749 (2005).
37. R. J. Lucas, S. Hattar, M. Takao, D. M. Berson, R. G. Foster, K. W. Yau, Diminished pupillary light reflex at high irradiances in melanopsin-knockout mice. *Science* **299**, 245–247 (2003).
38. A. Delwig, S. Y. Chaney, A. S. Bertke, J. Verweij, S. Quirce, D. D. Larsen, C. Yang, E. Buhr, R. Van Gelder, J. Gallar, T. Margolis, D. R. Copenhagen, Melanopsin expression in the cornea. *Vis. Neurosci.* **35**, E004 (2018).
39. L. D. Salay, A. D. Huberman, Divergent outputs of the ventral lateral geniculate nucleus mediate visually evoked defensive behaviors. *Cell Rep.* **37**, 109792 (2021).
40. G. E. Pickard, K.-F. So, M. Pu, Dorsal raphe nucleus projecting retinal ganglion cells: Why Y cells? *Neurosci. Biobehav. Rev.* **57**, 118–131 (2015).
41. R. Yehuda, D. Boisoneau, J. W. Mason, E. L. Giller, Glucocorticoid receptor number and cortisol excretion in mood, anxiety, and psychotic disorders. *Biol. Psychiatry* **34**, 18–25 (1993).
42. Q. Wei, H. M. Fentress, M. T. Hoversten, L. Zhang, E. K. Hebda-Bauer, S. J. Watson, A. F. Seasholtz, H. Akil, Early-life forebrain glucocorticoid receptor overexpression increases anxiety behavior and cocaine sensitization. *Biol. Psychiatry* **71**, 224–231 (2012).
43. L. S. Novaes, N. B. Dos Santos, R. F. P. Batalhote, M. B. Malta, R. Camarini, C. Scavone, C. D. Munhoz, Environmental enrichment protects against stress-induced anxiety: Role of glucocorticoid receptor, ERK, and CREB signaling in the basolateral amygdala. *Neuropharmacology* **113**, 457–466 (2017).
44. K. Y. Wong, A retinal ganglion cell that can signal irradiance continuously for 10 hours. *J. Neurosci.* **32**, 11478–11485 (2012).
45. J. Johnson, V. Wu, M. Donovan, S. Majumdar, R. C. Renteria, T. Porco, R. N. Van Gelder, D. R. Copenhagen, Melanopsin-dependent light avoidance in neonatal mice. *Proc. Natl. Acad. Sci. U.S.A.* **107**, 17374–17378 (2010).

46. W. T. Keenan, A. C. Rupp, R. A. Ross, P. Somasundaram, S. Hiriyanna, Z. Wu, T. C. Badea, P. R. Robinson, B. B. Lowell, S. S. Hattar, A visual circuit uses complementary mechanisms to support transient and sustained pupil constriction. *eLife* **5**, e15392 (2016).
47. F. Muindi, J. M. Zeitzer, D. Colas, H. C. Heller, The acute effects of light on murine sleep during the dark phase: Importance of melanopsin for maintenance of light-induced sleep. *Eur. J. Neurosci.* **37**, 1727–1736 (2013).
48. M. L. Aranda, T. M. Schmidt, Diversity of intrinsically photosensitive retinal ganglion cells: Circuits and functions. *Cell. Mol. Life Sci.* **78**, 889–907 (2021).
49. K. B. Sondereker, M. E. Stabio, J. M. Renna, Crosstalk: The diversity of melanopsin ganglion cell types has begun to challenge the canonical divide between image-forming and non-image-forming vision. *J. Comp. Neurol.* **528**, 2044–2067 (2020).
50. N. Milosavljevic, R. Storchi, C. G. Eleftheriou, A. Colins, R. S. Petersen, R. J. Lucas, Photoreceptive retinal ganglion cells control the information rate of the optic nerve. *Proc. Natl. Acad. Sci. U.S.A.* **115**, E11817–E11826 (2018).
51. D. M. Berson, A. M. Castrucci, I. Provencio, Morphology and mosaics of melanopsin-expressing retinal ganglion cell types in mice. *J. Comp. Neurol.* **518**, 2405–2422 (2010).
52. W. Y. Chen, X. Han, L. J. Cui, C. X. Yu, W. L. Sheng, J. Yu, F. Yuan, Y. M. Zhong, X. L. Yang, S. J. Weng, Cell-subtype-specific remodeling of intrinsically photosensitive retinal ganglion cells in streptozotocin-induced diabetic mice. *Diabetes* **70**, 1157–1169 (2021).
53. L. J. Cui, W. H. Chen, A. L. Liu, X. Han, S. X. Jiang, F. Yuan, Y. M. Zhong, X. L. Yang, S. J. Weng, nGnG amacrine cells and Brn3b-negative M1 ipRGCs are specifically labeled in the ChAT-ChR2-EYFP mouse. *Invest. Ophthalmol. Vis. Sci.* **61**, 14 (2020).
54. S. K. Chen, T. C. Badea, S. Hattar, Photoentrainment and pupillary light reflex are mediated by distinct populations of ipRGCs. *Nature* **476**, 92–95 (2011).
55. T. M. Schmidt, P. Kofuji, Differential cone pathway influence on intrinsically photosensitive retinal ganglion cell subtypes. *J. Neurosci.* **30**, 16262–16271 (2010).
56. A. L. Liu, Y. F. Liu, G. Wang, Y. Q. Shao, C. X. Yu, Z. Yang, Z. R. Zhou, X. Han, X. Gong, K. W. Qian, L. Q. Wang, Y. Y. Ma, Y. M. Zhong, S. J. Weng, X. L. Yang, The role of ipRGCs in ocular growth and myopia development. *Sci. Adv.* **8**, eabm9027 (2022).
57. M. Davis, The role of the amygdala in fear and anxiety. *Annu. Rev. Neurosci.* **15**, 353–375 (1992).
58. C. Beier, Z. Zhang, M. Yurgel, S. Hattar, Projections of ipRGCs and conventional RGCs to retinorecipient brain nuclei. *J. Comp. Neurol.* **529**, 1863–1875 (2021).
59. C. A. Vadnie, K. A. Petersen, L. A. Eberhardt, M. A. Hildebrand, A. J. Cerwensky, H. Zhang, J. N. Burns, D. D. Becker-Krail, L. M. DePoy, R. W. Logan, C. A. McClung, The suprachiasmatic nucleus regulates anxiety-like behavior in mice. *Front. Neurosci.* **15**, 765850 (2022).
60. E. W. Lamont, B. Robinson, J. Stewart, S. Amir, The central and basolateral nuclei of the amygdala exhibit opposite diurnal rhythms of expression of the clock protein Period2. *Proc. Natl. Acad. Sci. U.S.A.* **102**, 4180–4184 (2005).
61. D. Caudal, T. M. Jay, B. P. Godsil, Behavioral stress induces regionally-distinct shifts of brain mineralocorticoid and glucocorticoid receptor levels. *Front. Behav. Neurosci.* **8**, 19 (2014).
62. J. K. Zavala, A. A. Fernandez, K. L. Gosselink, Female responses to acute and repeated restraint stress differ from those in males. *Physiol. Behav.* **104**, 215–221 (2011).
63. M. N. Vitousek, C. C. Taff, D. R. Ardia, J. M. Stedman, C. Zimmer, T. C. Salzman, D. W. Winkler, The lingering impact of stress: Brief acute glucocorticoid exposure has sustained, dose-dependent effects on reproduction. *Proc. Biol. Sci.* **285**, 20180722 (2018).
64. M. Joëls, Corticosteroids and the brain. *J. Endocrinol.* **238**, R121–R130 (2018).
65. E. D. Leonardo, R. Hen, Anxiety as a developmental disorder. *Neuropsychopharmacology* **33**, 134–140 (2008).
66. L. K. Fonken, R. J. Nelson, Dim light at night increases depressive-like responses in male C3H/HeNHsd mice. *Behav. Brain Res.* **243**, 74–78 (2013).
67. T. A. Bedrosian, Z. M. Weil, R. J. Nelson, Chronic dim light at night provokes reversible depression-like phenotype: Possible role for TNF. *Mol. Psychiatry* **18**, 930–936 (2013).
68. T. A. Bedrosian, L. K. Fonken, J. C. Walton, A. Haim, R. J. Nelson, Dim light at night provokes depression-like behaviors and reduces CA1 dendritic spine density in female hamsters. *Psychoneuroendocrinology* **36**, 1062–1069 (2011).
69. L. K. Fonken, M. S. Finy, J. C. Walton, Z. M. Weil, J. L. Workman, J. Ross, R. J. Nelson, Influence of light at night on murine anxiety- and depressive-like responses. *Behav. Brain Res.* **205**, 349–354 (2009).
70. L. P. Morin, K. M. Studholme, Millisecond light pulses make mice stop running, then display prolonged sleep-like behavior in the absence of light. *J. Biol. Rhythms* **24**, 497–508 (2009).
71. P. Badia, B. Myers, M. Boecker, J. Culpepper, J. R. Harsh, Bright light effects on body temperature, alertness, EEG and behavior. *Physiol. Behav.* **50**, 583–588 (1991).
72. J. L. Ecker, O. N. Dumitrescu, K. Y. Wong, N. M. Alam, S. K. Chen, T. LeGates, J. M. Renna, G. T. Prusky, D. M. Berson, S. Hattar, Melanopsin-expressing retinal ganglion-cell photoreceptors: Cellular diversity and role in pattern vision. *Neuron* **67**, 49–60 (2010).
73. T. A. Legates, D. Dunn, E. T. Weber, Accelerated re-entrainment to advanced light cycles in BALB/cJ mice. *Physiol. Behav.* **98**, 427–432 (2009).
74. X. H. Wu, K. W. Qian, G. Z. Xu, Y. Y. Li, Y. Y. Ma, F. Huang, Y. Q. Wang, X. Zhou, J. Qu, X. L. Yang, Y. M. Zhong, S. J. Weng, The role of retinal dopamine in C57BL/6 mouse refractive development as revealed by intravitreal administration of 6-hydroxydopamine. *Invest. Ophthalmol. Vis. Sci.* **57**, 5393–5404 (2016).
75. A. Ishida, T. Mutoh, T. Ueyama, H. Bando, S. Masubuchi, D. Nakahara, G. Tsujimoto, H. Okamura, Light activates the adrenal gland: timing of gene expression and glucocorticoid release. *Cell Metab.* **2**, 297–307 (2005).

Acknowledgments: We thank T. Xue (University of Science and Technology of China) for providing *Opn4*$^{-/-}$ and *rd/rd cl* mice, S. Hattar (National Institute of Mental Health) for providing *Opn4*$^{Cre/+}$ mice, and X. Xiao (Fudan University) for assistance in behavioral data analysis. **Funding:** This work was supported by STI 2030-Major Projects (2022ZD0208604 and 2022ZD0208605), the National Natural Science Foundation of China (81790640, 82070993, 31571072, 32070989, 31872766, and 31571075), Shanghai Municipal Science and Technology Major Project (no. 2018SHZDZX01), ZJLab, Shanghai Center for Brain Science and Brain-Inspired Technology, and Sanming Project of Medicine in Shenzhen (SZSM202011015). **Author contributions:** Experiment design: S.-J.W. and G.W. Experiment administration: G.W., Y.-F.L., Z.Y., C.-X.Y., Q.T., Y.-L.T., Y.-Q.S., X.X., and L.-Q.W. Data analysis: G.W., Y.-M.Z., S.-J.W., X.X., H.C., and Y.-Q.Z. Writing: X.-L.Y., S.-J.W., Y.-M.Z., and G.W. **Competing interests:** The authors declare that they have no competing interests. **Data and materials availability:** All data needed to evaluate the conclusions in the paper are present in the paper and/or the Supplementary Materials. *Opn4*$^{Cre/+}$ mice are available from S. Hattar (samer.hattar@nih.gov) under a material transfer agreement with National Institute of Mental Health, and *Opn4*$^{-/-}$ and *rd/rd cl* mice are available from T. Xue (xuetian@ustc.edu.cn) under a material transfer agreement with University of Science and Technology of China.

Submitted 29 October 2022
Accepted 17 February 2023
Published 22 March 2023
10.1126/sciadv.adf4651